# Experimental Investigation of Straight and Curved Annular Wall Jets

L. C. Rodman,* N. J. Wood,† and L. Roberts‡
*Stanford University, Stanford, California*

**Accurate turbulence measurements taken in wall jet flows are difficult to obtain, due to high-intensity turbulence and problems in achieving two-dimensionality. The problem is compounded when streamwise curvature of the flow is introduced, due to higher jet entrainment and turbulence levels. In this experiment, two-dimensional straight and curved wall jet flows were simulated by having a jet blow axially over a cylinder. Although the wall jet in these cases is annular, adequate "two-dimensional" flow can be obtained as long as the ratio of the jet width to the cylinder radius is small. With an annular wall jet, three-dimensional effects are caused by the finite length of the slot and sidewall interference are eliminated. Hot-wire measurements are presented for straight and curved wall jets, and an integral analysis is used to assess the effects of transverse curvature on the flowfield. The analysis and the data show that the effects of transverse curvature on both the mean flow and turbulent shear stress are small in the upstream portions of the wall jet, and two-dimensional flow is satisfactorily approximated. However, transverse curvature effects increase. A criterion is established to delineate the region of validity and to aid in designing future annular models.**

## Nomenclature

$a$ = constant in eddy viscosity equation
$b$ = wall jet half-width, position where $U = U_m/2$
$C_f$ = skin-friction coefficient
$f$ = self-similar velocity profile function $U/U_m$
$h$ = jet slot height
$h$ = $r/r_0$ in integral momentum analysis
$K$ = planar wall jet growth rate
$M(x)$ = jet momentum as a function of downstream coordinate $x$
$M_0$ = jet momentum issuing from slot
$n$ = constant in velocity profile
$r$ = radial coordinate in axisymmetric flow, $r = r_0 + y\cos\phi$
$r_0$ = radial coordinate describing the surface of axisymmetric model
$R$ = local streamwise radius of curvature
$u,v$ = streamwise, normal velocity component
$U$ = mean streamwise velocity component
$U_j$ = jet exit velocity
$U_m$ = maximum mean streamwise velocity at a given $x$
$\overline{u'^2}$ = time mean square of fluctuating $u$ component
$\overline{u'v'}$ = turbulent shear stress
$\overline{v'^2}$ = time mean square of fluctuating $v$ component
$x_0$ = jet virtual origin
$x,y$ = streamwise, normal coordinates
$\xi$ = normalized coordinate, $= y/b$
$\xi_m$ = position of the maximum velocity
$\epsilon$ = eddy viscosity
$\kappa$ = constant in velocity profile
$\rho$ = density
$\tau$ = shear stress, $= \mu du/dy - \rho\overline{u'v'}$
$\phi$ = angular position along circular arc

## Introduction

A WALL jet is a thin jet of fluid blown tangentially along a wall, where the surrounding fluid may be either at rest or coflowing. The wall jet resembles half of a free jet with a wall boundary layer imposed, and in most practical applications the wall jet will be fully turbulent. The adjacent wall may be either straight or have streamwise curvature.

One of the most interesting and useful features of the wall jet is the Coanda effect, whereby the jet remains strongly attached to a convex surface. Curved wall jets also display an increase in their mixing with the surrounding fluid compared with straight wall jets. These two properties (wall attachment and increased mixing) enable the wall jet to delay separation of an external stream from a curved surface. Accordingly, curved wall jets have the most use in aeronautical applications, where blowing is used to delay separation from the upper surface of an airfoil.

Many experiments have been performed to study the turbulence structure of two-dimensional wall jets and, since wall jets display characteristics of both free shear flows and wall-bounded flows, they are an interesting test case for turbulence models. In particular, the location of the zero mean velocity gradient does not correspond to the location of zero turbulent shear stress, thus standard mixing length models do not accurately predict the shear profile of a wall jet. Wall jets over straight walls achieve some degree of self-similarity, which may simplify their calculation. If the wall is curved, however, similarity will only occur if the ratio of the streamwise coordinate to the radius of curvature remains constant, i.e., for a logarithmic spiral.

Accurate measurements have been difficult to obtain in wall jet flows, due to high-intensity turbulence and the complexity of achieving satisfactory two-dimensional flow. If the span of the slot is finite, vorticity is created at the slot ends, which propagates toward the centerline, producing three-dimensional effects. The problem is compounded when streamwise

Received Nov. 23, 1987; revision received Sept. 27, 1988. 

*Graduate Research Assistant, Department of Aeronautics and Astronautics, presently Research Scientist, Nielsen Engineering and Research, Inc. Member AIAA.

†Research Associate, Department of Aeronautics and Astronautics. Member AIAA.

‡Professor, Department of Aeronautics and Astronautics. Fellow AIAA.

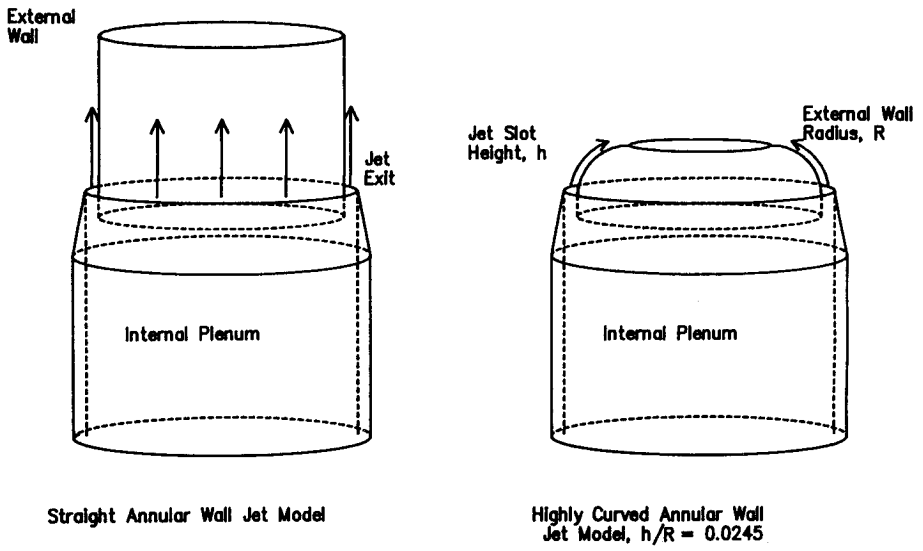


**Fig. 1 Annular wall jet models.**

curvature of the flow is introduced, since the jet entrainment and turbulence levels are greatly increased over the equivalent planar values. Nonuniformity of the slot along the span also has been shown to decrease the flow quality. To reduce three-dimensional effects, the jet slot should have a very large aspect ratio, yet most practical experiments have been constrained by physical size or volume flow limitations. To date, most of the measurements published have been affected by inadequate two-dimensionality, as assessed by momentum conservation techniques.[1]

The objective of the present work was to obtain a set of detailed turbulence measurements in straight and curved wall jets in still air and to achieve a flow quality as close to two-dimensional as possible. To reduce three-dimensional effects, an annular wall jet model was developed, with the jet blown axially along the outside of a body of revolution (Fig. 1). The ratio of the jet slot height $h$ to the cylinder radius was small (0.6%), so that transverse curvature effects were expected to be negligible. The thin annular jet around the body of revolution eliminated and effects, and the slot was easier to produce accurately and uniformly compared to a more conventional rectangular slot.

With the addition of streamwise curvature to a cylindrical model, the flow becomes more complex since the annular radius is no longer constant. An integral momentum technique was developed to predict the effects of transverse curvature on the wall jet, and the results for the annular curved wall jet were compared with those for the two-dimensional curved wall jet.

## Description of Experiment

The annular wall jet model was designed so that transverse curvature effects were minimized. The model consisted of two cylinders (Fig. 1). The larger, outer cylinder housed the plenum chamber and formed the slot lip of the nozzle. The volume of the chamber was large enough for the flow to settle and to remove circumferential nonuniformities. The slightly smaller, inner cylinder formed the wall for the jet. Three wall cylinders were constructed and were easily interchangeable. Both cylinders were independently supported by a central tube, which eliminated any need for a suport structure within the contraction and allowed a cleaner exit flow.

One of the three walls developed for this experiment was straight, and the other two were curved. The straight wall was a cylinder with a radius of approximately 20 cm. The slot height was 1.3 mm, and the slot lip was 0.25 mm thick at the edge. The wall extended 23 cm downstream, or approximately 180 slot heights. With a jet exit velocity of 100 m/s, the Reynolds number based on slot height was 9000.

Both of the curved walls had a constant radius of curvature in the streamwise direction, making them circular arcs. One of the walls was mildly curved, with a slot height: radius of curvature ratio $h/R$ of 0.0031. The ratio was chosen to match that of a previously published two-dimensional wall jet experiment.[2] The other wall had a much stronger curvature, with $h/R = 0.0290$. The walls curved in toward the center, so that the cylinder radius decreased with downstream distance. The cylinder radius at the slot was the same for all three walls.

Measurements in the flow were made using cross-wire anemometry. A digital calibration of the hot-wire signals was made using a King's law curve fit; a complete description of this technique is given in Ref. 3. Profiles of the mean velocity and the turbulence quantities were taken at various downstream stations. The turbulence quantities measured were the three Reynolds stress components $\overline{u'^2}$, $\overline{v'^2}$, and $\overline{u'v'}$, as as well as selected triple components. The mean flow and shear stress measurements will be discussed in this paper. Presentation of the other measured turbulence quantities and a complete description of the experimental apparatus may be found in Ref. 3.

## Results

### Mean Flow Results

Pitot tube measurements taken along the circumference of all three models showed good flow uniformity and "two-dimensionality" along the jet span. Both a two-dimensional and an axisymmetric momentum equation check were used to assess two-dimensionality in the straight wall jet.[1] In a two-dimensional flow, loss of streamwise momentum should be small since it is due only to skin friction. Thus, the ratio of jet momentum $M(x)$ relative to the slot momentum $M_0$ is for a two-dimensional flow

$$\frac{M(x)}{M_0} = \left(\frac{U_m}{U_j}\right)^2 \frac{b}{h} \int_0^\infty \left(\frac{U}{U_m}\right)^2 d\xi \tag{1}$$

and for an axisymmetric flow

$$\frac{M(x)}{M_0} = \left(\frac{U_m}{U_j}\right)^2 \frac{b}{h} \int_0^\infty \frac{r}{r_0}\left(\frac{U}{U_m}\right)^2 d\xi \tag{2}$$

where $r$ is the annular radial coordinate, $r_0$ the surface of the model, $b$ the jet half-width, $U_m$ the local maximum velocity, and $\xi$ the normal distance from the wall normalized by the jet half-width. In two-dimensional flow along a frictionless wall, $M(x)/M_0 = 1$ for all $x$. In actuality, the ratio decreases slowly

with distance downstream. For this flow using (1), the momentum ratio ranged from 0.89 to 0.76 and with Eq. (2) from 0.90 to 0.77. The difference was less than 3% between the two calculations, and they both showed adequate conservation of momentum in the streamwise direction.

The two-dimensional straight wall jet is a self-similar flow, and the profiles in Fig. 2 indicated that the annular straight wall jet was also self-similar. The dotted line shows a two-dimensional velocity profile from Ref. 4, which is representative of previous straight wall jet experiments. There was virtually no difference between the current annular profiles and the previous two-dimensional profiles.

Curved wall jets are self-similar only if the ratio of the wall radius of curvature is proportional to the distance downstream, as with a logarithmic spiral. Although wall jets over circular arcs (constant radius of curvature) are not strictly self-similar, the mean flow changes slowly enough downstream that the self-similar approximation is valid. The mildly curved wall jet had velocity profiles that were identical to the straight wall case. Only for the highly curved wall jet (Fig. 3) could any variation in the velocity profiles be seen with downstream distance, but the change was still slight. Figure 3 also shows a comparison with the data for the straight wall jet model. The highly curved velocity profile had a slightly fuller profile above the velocity maximum. This difference was seen in two-dimensional wall jets as well.[4]

Figure 4 shows the straight annular wall jet growth rate plotted with two-dimensional data from previous researchers. Except for a shift in the virtual origin that varies from experiment to experiment, the annular jet grew at the same rate as previously measured rectangular jets, with a linear growth rate[1] equal to 0.073. Similar plots of the jet growth rates for curved wall jets are shown in Fig. 5. Curved wall jets display enhanced mixing relative to straight wall jets, and this is shown by the increased growth rates of these jets. As the curvature of the jet increases, the growth rate also increases. Correspondingly, the decay rate of the maximum velocity increases as well. The annular data showed the same trends as previous two-dimensional results.

### Turbulence Results

The turbulence quantities of interest in wall jet flows are the Reynolds stresses, in particular the shear stress $\overline{u'v'}/U_m^2$. These stresses are normalized by the local mean maximum velocity. Although the normal stresses $\overline{u'^2}/U_m^2$ and $\overline{v'^2}/U_m^2$ are also of interest, the shear stress is the term that needs to be modeled in a calculation scheme.

Figure 6 shows the Reynolds shear stress profiles as they changed downstream for the annular straight wall jet. The profiles were nearly self-similar with downstream distance, with only a slight growth seen. Figure 6 also shows a bandwidth indicating previous results.[1] The profile shapes agreed with previous two-dimensional data; however, the peak shear stress in the present experiment was lower than the peak shear obtained by previous researchers.

Reynolds stress profiles for the curved wall jets are shown in Figs. 7 and 8. These plots demonstrated that the degree of self-similarity of the normalized turbulent quantities decreased as the streamwise curvature increased. The results for the mildly curved wall jet were similar to those of the straight wall, although a slightly higher growth of the peak intensities could be seen. In the highly curved wall jet, this growth was more clearly indicated, showing that, although the mean flow was close to self-similar, the turbulence field was not.

The results of the experimental investigation have shown the effects of streamwise curvature on the mean and turbulent wall jet flowfield, and these effects are summarized here. The mean velocity profiles were found to be invariant with downstream location for both the straight and curved wall jets, although the highly curved jet profile was slightly fuller near the velocity maximum. Curvature strongly affected the growth rate of the jet half-width, causing it to increase with higher curvature.

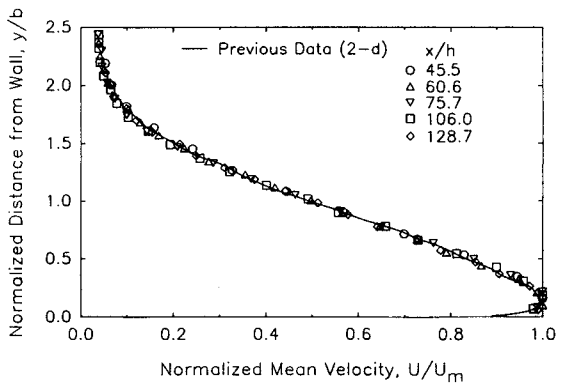


**Fig. 2 Self-similar mean velocity profiles in the straight annular wall jet (cross-wire measurements).**

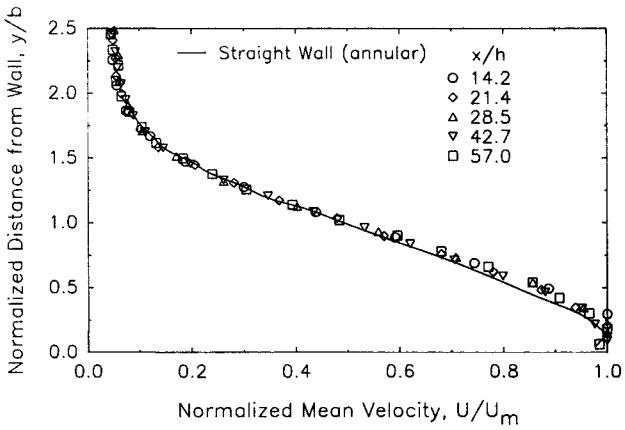


**Fig. 3 Self-similar mean velocity profiles in the highly curved annular wall jet (cross-wire measurements).**

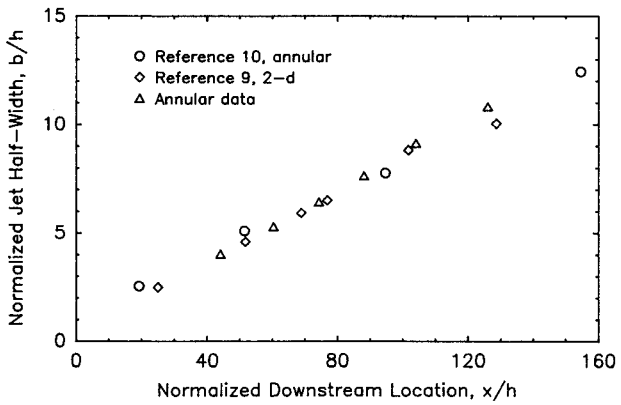


**Fig. 4 Half-width growth in the straight annular wall jet.**

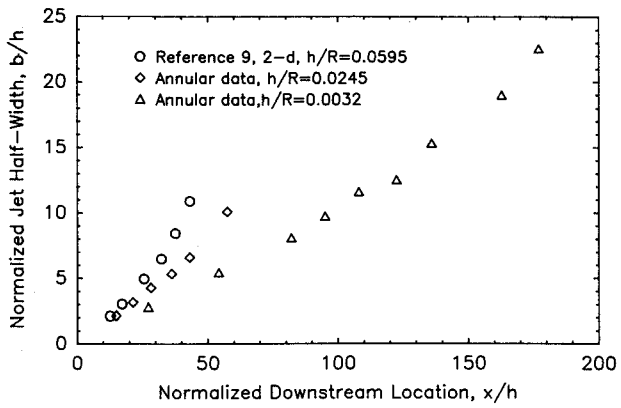


**Fig. 5 Half-width growth in curved annular wall jets.**

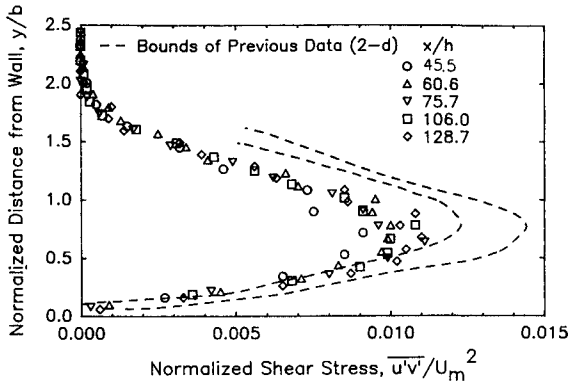


**Fig. 6 Shear stress profiles in the straight annular wall jet (cross-wire measurements).**

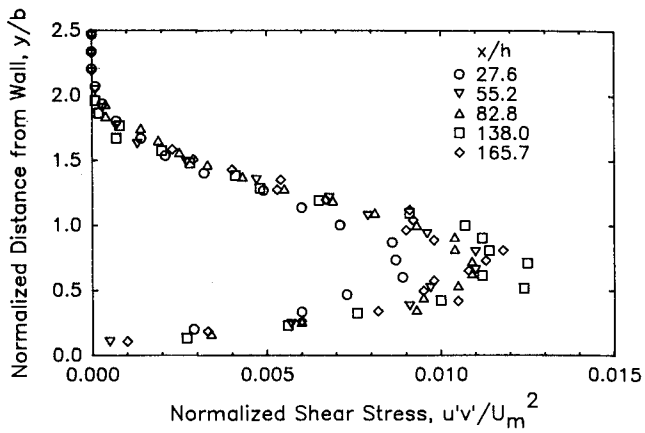


**Fig. 7 Shear stress profiles in the mildly curved annular wall jet (cross-wire measurements).**

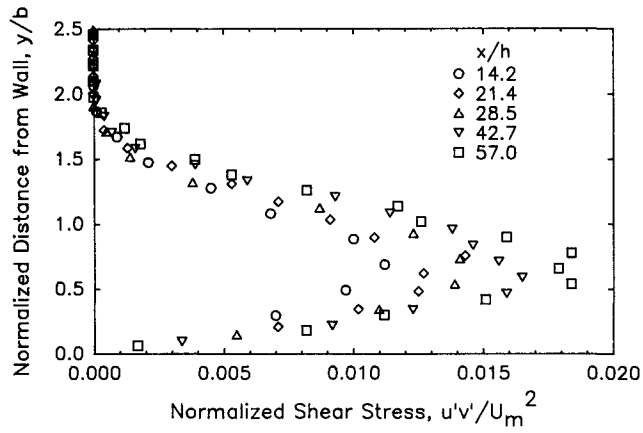


**Fig. 8 Shear stress profiles in the highly curved annular wall jet (cross-wire measurements).**

There did not seem to be an appreciable difference between the annular mean flow data and data from previous rectangular experiments.

The Reynolds stress profiles showed self-similarity in the straight wall jet, but the turbulence quantities were increased relative to the mean flow in the curved jets. This same trend was seen for all three Reynolds stresses. The Reynolds stress profiles taken in the annular models followed trends similar to previous data taken in rectangular models. The one exception was the magnitude of the peak shear stress, which was slightly lower in the annular experiment.

## Analysis

An integral analysis was developed to predict the effects of transverse curvature on the mean flow and turbulent shear stress in curved wall jets. The analysis was originally developed for two-dimensional curved wall jets[5] and was extended to the axisymmetric case of a wall jet over a curved body of revolution.

Integral methods are used in flows for which a self-similar velocity profile may be assumed. Since the normalized velocity profile can be expressed easily in functional form, the momentum equation may be integrated directly to obtain the shear stress. For wall jets, the self-similar velocity profile is obtained by normalizing the velocities and lengths by the local maximum velocity $U_m(x)$ and the local jet half-width $b(x)$, respectively. Thus, it is necessary to solve for the downstream development of both $U_m$ and $b$ in order to completely determine the mean velocity field in the flow. Two equations were found in terms of the jet growth rate $db/dx$ and the rate of change of the momentum flux $d(bU_m^2)/dx$. A marching scheme was used to solve these differential equations along the streamwise direction, thus allowing the solution of $U_m$, $b$, and the shear stress profile to be found at each $x$ location.

The thin shear layer equations of motion for a wall jet over a body of revolution were used.[6] The differential form of these equations was

Mass:
$$\frac{\partial(ru)}{\partial x} + \frac{\partial(rv)}{\partial y} = 0 \tag{3}$$

$x$ momentum:
$$u\frac{\partial u}{\partial x} + v\frac{\partial u}{\partial y} = -\frac{1}{\rho}\frac{\partial p}{\partial x} + \frac{1}{\rho r}\frac{\partial(r\tau)}{\partial y} \tag{4}$$

$y$ momentum:
$$\frac{u^2}{R} = \frac{1}{\rho}\frac{\partial p}{\partial y} \tag{5}$$

In this notation, $x$ and $y$ are curvilinear coordinates that follow the wall and $r$ is the distance to the axis of revolution (Fig. 9),

$$r(x,y) = r_0(x) + y\cos\phi(x) \tag{6}$$

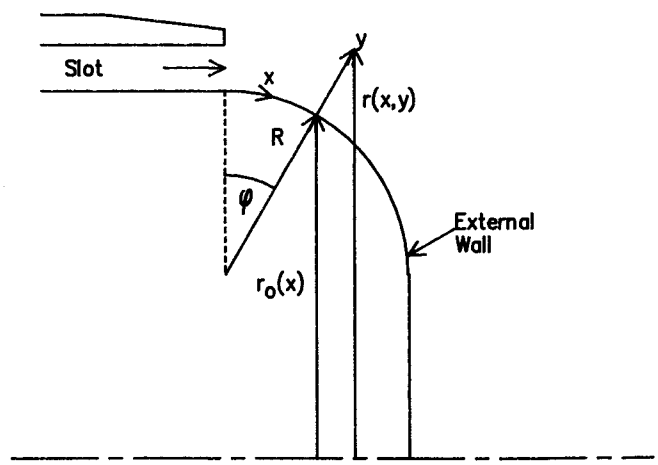


**Fig. 9 Coordinate system for a body of revolution.**

Note that neither the slope of the surface nor the angle $\phi$ need to be small for this analysis. For a straight wall, $r_0$ is constant, and $\phi$ is everywhere equal to zero, so $r$ is a function of $y$ only. If then the jet is thin compared to the radius of the cylinder, $d(r/r_0)/dy$ is approximately zero, and the equations reduce to the two-dimensional plane equations. For curved flows, $R$ is the local streamwise radius of curvature, as in the two-dimensional equations. In the following analysis, $r$ was retained as a function of $x$ and $y$, and $R$ was an arbitrary function of $x$. By letting $h = r/r_0$ and combining $u$ times Eq. (3) and $r$ times Eq.

(4), the integral momentum equation also can be written (with $y'$ the variable of integration for clarity) as

$$\int_y^\infty \frac{1}{r_0}\frac{\partial(u^2 r)}{\partial x}\,dy' + \int_y^\infty \frac{\partial(huv)}{\partial y'}\,dy' = \int_y^\infty -\frac{h}{\rho}\frac{\partial p}{\partial x}\,dy' + \int_y^\infty \frac{1}{\rho}\frac{\partial(h\tau)}{\partial y'}\,dy' \tag{7}$$

In order to take advantage of the self-similar profile $U/U_m = f(\xi)$, where $f(\xi)$ vanishes at $\xi = 0$ and is assumed to decay exponentially as $\xi$ goes to infinity, a new coordinate system $(x, \xi)$ was used where $\xi = y/b(x)$, with the transformation

$$\frac{d}{dx} = \frac{\partial}{\partial x} - \left(\frac{\xi}{b}\right)\frac{db}{dx}\frac{\partial}{\partial \xi}$$

$$\frac{d}{dy} = \left(\frac{1}{b}\right)\frac{\partial}{\partial \xi}$$

Then, the substitution of the mean velocity profile and Eq. (6) into Eq. (7) and the assumption that the jet is thin compared with both the streamwise and annular radii of curvature, so terms arising from the pressure gradients of $O(b/R)^2$ and $(b/r_0)^2$ can be neglected, yielded the final equation for the shear stress (with $\xi'$ the variable of integration for clarity):

$$C_1\int_\xi^\infty f^2\,d\xi' + C_2\int_\xi^\infty \xi' f^2\,d\xi' + C_3\frac{1}{2}f\int_0^\infty f\,d\xi' + C_4 f\int_0^\infty \xi' f\,d\xi' + C_5\,\xi\int_\xi^\infty f^2\,d\xi' = -\frac{r}{r_0}\frac{\tau}{\rho U_m^2} \tag{8}$$

where

$$C_1 = \frac{b}{r_0}\frac{dr_0}{dx} + \frac{1}{U_m^2}\frac{d(bU_m^2)}{dx}$$

$$C_2 = \left(\frac{1}{U_m^2}\frac{d(bU_m^2)}{dx} + \frac{db}{dx}\right)\left(\frac{b}{r_0}\cos\phi - \frac{b}{R}\right) - \frac{b}{r_0}\,b\sin\phi\frac{d\phi}{dx} + \frac{b^2}{R^2}\frac{dR}{dx}$$

$$C_3 = \left(\frac{1}{U_m^2}\frac{d(bU_m^2)}{dx} + \frac{db}{dx}\right) + 2\frac{b}{r_0}\frac{dr_0}{dx}$$

$$C_4 = \frac{b}{r_0}\cos\phi\left(\frac{1}{2}\frac{1}{U_m^2}\frac{d(bU_m^2)}{dx} + \frac{3}{2}\frac{db}{dx}\right) - \frac{b}{r_0}\sin\phi\frac{d\phi}{dx}\,b$$

$$C_5 = \frac{b}{R}\frac{1}{U_m^2}\frac{d(bU_m^2)}{dx} - \frac{b^2}{R^2}\frac{dR}{dx}$$

Note that terms involving $(dR/dx)(b/R)^2$ were kept since the axial growth of the mean flow, $dU_m/dx$ and $db/dx$, were assumed to be small as well.

The two equations necessary to solve for the growth rate and the rate of change of momentum flux were obtained by evaluating Eq. (8) at $\xi = 0$ and by evaluating the transformed Eq. (4) at $\xi = \xi_m$.

The evaluation of Eq. (8) at $\xi = 0$ yielded

$$\left(\frac{1}{U_m^2}\frac{d(bU_m^2)}{dx} + \frac{b}{r_0}\frac{dr_0}{dx}\right)A_n + \left(\cos\phi - \frac{r_0}{R}\right)\left(\frac{1}{U_m^2}\frac{d(bU_m^2)}{dx} + \frac{db}{dx}\right)\frac{b}{r_0}C_n + \left(\frac{r_0^2}{R^2}\frac{dR}{dx} - r_0\sin\phi\frac{d\phi}{dx}\right)\frac{b^2}{r_0^2}C_n = -\frac{1}{2}C_f \tag{9}$$

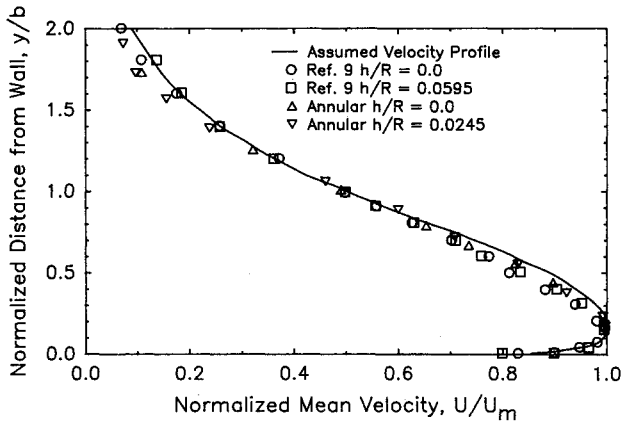


**Fig. 10 Assumed self-similar velocity profile.**

where

$$A_n = \int_0^\infty f^2\,d\xi$$

$$C_n = \int_0^\infty \xi f^2\,d\xi$$

The assumed self-similar velocity profile was given by the following functions:

$$\frac{U}{U_m} = 2\left(\frac{\xi}{\xi_m}\right)^{1/n} - \left(\frac{\xi}{\xi_m}\right)^{2/n} = f(\xi), \qquad \xi \le \xi_m$$

$$\frac{U}{U_m} = \operatorname{sech}^2\frac{\kappa(\xi - \xi_m)}{(1 - \xi_m)} = f(\xi), \qquad \xi \ge \xi_m \tag{10}$$

where $\xi_m$ is the position of the maximum velocity. The form of these functions ensures that $f(\xi_m) = 1$ and $f'(\xi_m) = 0$. The first function gave the velocity profile for the inner region of the jet. The power law form was suggested by the relation for turbulent boundary layers. Typical values of the exponent $n$ for boundary layer flows were 6 or 7. The second relationship, for the outer region of the flow, came directly from the solution for a turbulent two-dimensional free jet. Both of the above functions have been written so that the maximum velocity occurred at $\xi = \xi_m$.

By setting $U/U_m = \frac{1}{2}$ at $\xi = 1$, the constant $\kappa$ was found to be 0.8814. Matching the second derivatives of the functions at $\xi = \xi_m$ gave $\xi_m = 1/(1 + nk) = 0.159$ when the value $n = 6$ was used. This compares well with the experimental value of 0.16 suggested by Wilson and Goldstein.[4] Figure 10 shows the assumed velocity profile, along with experimental data for the straight wall jet. The two profiles agreed fairly well everywhere except for a small region outer of the velocity maximum, where the assumed profile was slightly fuller than the experimental profile.

Assuming $n$ was large and $C_f \to 0$ (valid for large Reynolds number flows) gave

$$A_n = \frac{2}{3\kappa}$$

$$C_n = \frac{2}{3\kappa}\left(\frac{\ell n 2 - \frac{1}{4}}{\kappa}\right)$$

$$\left[1 + \left(\cos\phi - \frac{r_0}{R}\right)\left(\frac{b}{r_0}\right)\left(\frac{\ell n 2 - \frac{1}{4}}{\kappa}\right)\right]\frac{1}{U_m^2}\frac{d(bU_m^2)}{dx} + \left[\left(\cos\phi - \frac{r_0}{R}\right)\frac{b}{r_0}\left(\frac{\ell n 2 - \frac{1}{4}}{\kappa}\right)\right]\frac{db}{dx} + \frac{b}{r_0}\frac{dr_0}{dx} + \left(\frac{r_0^2}{R^2}\frac{dR}{dx} - r_0\sin\phi\frac{d\phi}{dx}\right)\left(\frac{\ell n 2 - \frac{1}{4}}{\kappa}\right)\frac{b^2}{r_0^2} = 0 \tag{11}$$

The second equation for the mean flowfield was found by evaluating Eq. (4) at $\xi = \xi_m$. This required the use of an approximation for the value of $\tau$ at $\xi_m$. Using an eddy viscosity approximation to be applied at $\xi = \xi_m$ and setting

$$\frac{\tau}{\rho} = \epsilon\left(\frac{\partial u}{\partial y} - \frac{u}{R}\right)$$

$$\epsilon = \frac{K}{4\kappa^2}(1 - \xi_m) b U_m g(\xi)$$

$$g(\xi) = (\xi/\xi_m)^m[(a + (1-a)\xi/\xi_m)]$$

it was found that $m = 1 - 1/n$ and $a = C_f\,\kappa/K$ in order to satisfy the condition that the shear stress equals the skin friction at the wall. Assuming $n$ was large and $C_f \to 0$ gave the final equation

$$\frac{db}{dx} = K\left[1 + \frac{b}{R}\frac{n}{\kappa}\right] + \frac{K}{2\kappa^2}\cos\phi\,\frac{b}{r_m}\frac{b}{R} + \left(1 - \frac{4}{3\kappa}\frac{b}{R}\right)\frac{1}{U_m^2}\frac{d(bU_m^2)}{dx} + \frac{4}{3\kappa}\frac{b^2}{R^2}\frac{dR}{dx} \tag{12}$$

where $r_m$ is the radial distance to $\xi_m$.

For a circular arc in the streamwise direction, $R$ = const and Eqs. (11) and (12) were simplified by substituting

$$\frac{d\phi}{dx} = \frac{1}{R}, \quad \phi = \frac{x}{R}$$

$$r_0(x) = r_0(0) - R(1 - \cos\phi)$$

$$\frac{dr_0}{dx} = -\sin\phi, \quad \frac{\ell n 2 - \frac{1}{4}}{\kappa} = 0.503$$

$$\cos\phi - \frac{r_0}{R} = 1 - \frac{r_0(0)}{R}$$

The equations were now written

$$\left(A\frac{b}{r_0}\right)\frac{db}{dx} + \left(1 + A\frac{b}{r_0}\right)\frac{1}{U_m^2}\frac{d(bU_m^2)}{dx} = -\frac{b}{r_0}\frac{dr_0}{dx}\left(1 + \frac{b}{R}C\right) \tag{13}$$

$$\frac{db}{dx} + \left(\frac{4}{3\kappa}\frac{b}{R} - 1\right)\frac{1}{U_m^2}\frac{d(bU_m^2)}{dx} = K\left(1 + \frac{b}{R}\frac{n}{\kappa}\right) \tag{14}$$

where $C = C_n/A_n = (\ell n 2 - \frac{1}{4})/\kappa = 0.503$ and $A = C[1 - r_0(0)/R]$.

For the simpler case of a plane axisymmetric wall jet or a two-dimensional curved wall jet, the functions $db/dx$ and $1/U_m^2\, d(bU_m^2)/dx$ were found to the leading approximation:

Axisymmetric plane

$$\frac{db}{dx} = K\left(1 - C\frac{b}{r_0}\right) \tag{15}$$

$$\frac{1}{U_m^2}\frac{d(bU_m^2)}{dx} = -C\frac{b}{r_0}K \tag{16}$$

Two-dimensional curved ($R$ = const)

$$\frac{1}{U_m^2}\frac{d(bU_m^2)}{dx} = 0 \tag{17}$$

or

$$\left(\frac{U_j^2}{U_m^2}\right) = \frac{b}{h}, \quad \frac{db}{dx} = K\left(1 + \frac{n}{\kappa}\frac{b}{R}\right) \tag{18}$$

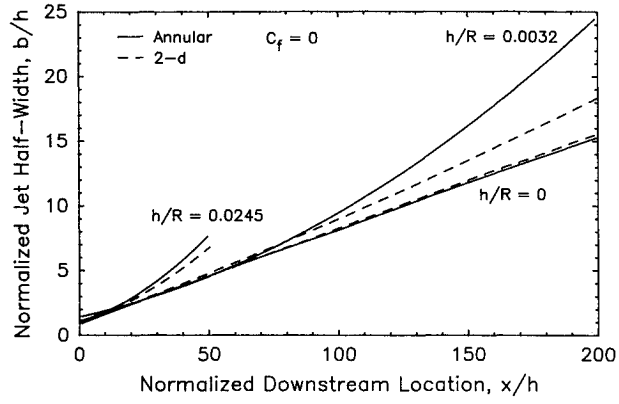


**Fig. 11 Computed annular and two-dimensional wall jet half-width growth.**

The empirical constant $K$ is the two-dimensional plane wall jet growth rate and is taken to be equal to 0.073 as suggested by previous research.[1]

Equation (14) reduced to the two-dimensional relation [Eq. (18)] if $1/U_m^2\, d(bU_m^2)/dx = 0$. In both equations, the rate of growth of the jet half-width had the same functional dependence on $b/R$. For a straight wall ($b/R = 0$), the growth rate was linear and equal to the constant $K$. The ratio $n/\kappa$ was approximately equal to 7; thus, the curvature term dominated the growth rate, even for small $b/R$. Equation (18) had an exact solution for $b$:

$$\frac{b}{h} = \frac{R}{h}\frac{\kappa}{n}\left[\exp\left(K\frac{n}{\kappa}\frac{x - x_0}{h}\frac{h}{R}\right) - 1\right]$$

which showed that curved wall jets grow at an exponential rate compared with a linear growth for a straight wall jet.

Equation (13) contained all of the transverse curvature effects in the mean flow equations. The transverse curvature appeared in the two quantities $b/r_0$ and $dr_0/dx$. As $b/r_0 \to 0$, Eq. (13) would reduce to the two-dimensional case.

Equations (13) and (14) were put into matrix form and solved for the two unknowns, $db/dx$ and $1/U_m^2\, d(bU_m^2)/dx$. The matrix equation was solved numerically by marching in the downstream direction. With the lengths $b$ and $x$ normalized by the slot height $h$ and $U_m^2$ normalized by the exit velocity squared $U_j^2$, the starting conditions were taken to be

$$U_m^2/U_j^2 = 1 \qquad x/h = 0$$

$$b/h = 1 \qquad x/h = 0 \tag{19}$$

The effect of streamwise curvature on the growth rates was clearly seen in both annular and two-dimensional flows (Fig. 11). The growth of the two-dimensional jet half-width was highly dependent on the streamwise curvature, due to centrifugal force effects on the mixing of the jet with the surrounding fluid. The analytical results, shown for $C_f = 0$, agreed with experimental results for both rectangular and annular flows. Since the initial condition that $b/h = 1$ at the slot was fixed in the analysis, it was expected that there might be some error in the intercept of the growth curve. Each experiment had associated with it a unique virtual origin that determined the intercept of its growth curve. The initial condition was chosen to be a general case, although an experimental value may be used instead. The initial condition also reflected the fact that the analysis assumed self-similar flow from the slot.

For both the annular and two-dimensional straight wall jets, the computed shear stress was self-similar. As streamwise curvature was introduced, the peaks grew downstream at a rate that increased as $h/R$ increased. The computed peak shear stress was about 70% higher than the measured shear stress in the straight wall flow.

The initial version of the computation was made assuming the skin-friction coefficient was equal to zero. The overprediction of peak shear stress led to an investigation of the effects of skin friction on the computational results. Since $C_f$ is a difficult quantity to measure, that measurement was not included in this experiment. A constant value of $C_f$ based on previous experiments was chosen for the purposes of the analysis.

The shear stress equation, Eq. (8), was invariant with skin friction, as it was derived. Since the term containing $C_f$ is negligible in Eq. (14), only Eq. (13) needed to be modified to include skin friction. The corrected Eq. (13) had the term $-\frac{1}{2}C_f/A_n$ added to the right-hand side.

In a further attempt to increase the accuracy of the integral method, the assumed velocity profiles used in the integrals in Eq. (8) were replaced by the experimental velocity profiles, which were integrated numerically. This correction was made because of the slight mismatch between the assumed and experimental velocity profiles (Fig. 10). When the velocity profile was integrated from the wall to the point of peak shear stress, the mismatch would cause the greatest error in the integral. The difference in peak values was significant. Since the velocity profiles for the highly curved wall jet was slightly fuller than the straight jet (Fig. 3), those velocity profiles matched the assumed profile, and the correction did not have a large effect.

The corrections were applied to the shear stress computation, and it was found that a value of $C_f = 0.013$ provided the best match to the experimental results. The corrected peak shear stress is shown in Fig. 12 for the straight annular model. Experimental results are also shown.

For the curved jets, the skin friction has been found to vary with streamwise curvature[7] by the relationship

$$C_f = C_{f_0}(1 + 2b/R) \tag{20}$$

where $C_{f_0}$ is the value for a straight wall. Choosing the value of $C_{f_0}$ which provided a match at the furthest upstream point, produced the curves shown in Figs. 13 and 14 for the mildly and highly curved jets. For the mildly curved wall jet, the use of the experimental velocity profiles reproduced the drop in shear stress at $x/h = 180$ seen in the data. Although the skin-friction coefficient increased with downstream location, the agreement between theory and experiment deteriorated in the highly curved wall jet. Apparently, the analysis cannot accurately compute the highly curved flows downstream, possibly because the streamwise derivatives were no longer negligible as was assumed in the thin shear layer approximation.

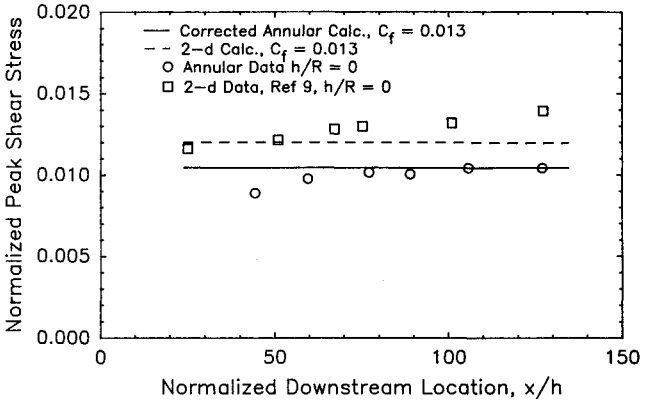


**Fig. 12 Comparison of annular and two-dimensional shear stress in the straight wall jet.**

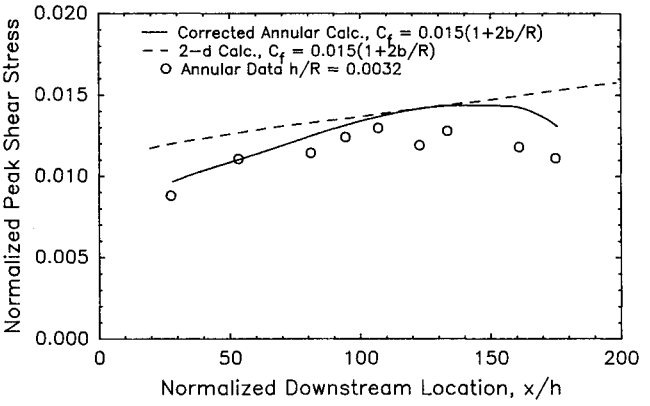


**Fig. 13 Comparison of annular and two-dimensional shear stress in mildly curved wall jets.**

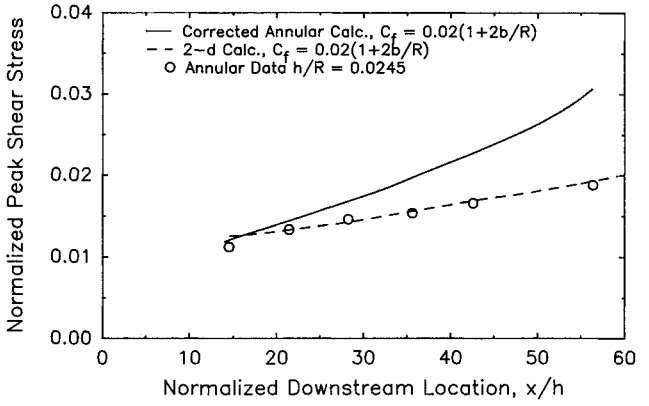


**Fig. 14 Comparison of annular and two-dimensional shear stress in highly curved wall jets.**

## Discussion

The objective of this research was to investigate experimentally the turbulence properties of a highly curved wall jet, while avoiding the problems with three-dimensionality faced by previous researchers. These problems include vorticity created at the slot ends and difficult machining. An annular wall jet model was used to approximate a two-dimensional flow with no end effects. This model was very successful in producing a uniform flow along the span. Easier machining and an improved contraction geometry were other advantages to this model.

The peak shear stress measured in the present experiment was in all cases about 25% lower than the peak shear stress obtained by previous researchers on rectangular models. Two possible explanations for this effect were that the transverse curvature in the flow decreased the shear stress in the annular jet or that the contraction flow in this particular model was clean enough to reduce the turbulence levels near the slot. The transverse curvature explanation seemed unlikely for several reasons. A test of the effect of transverse curvature was performed by comparing shear stress profiles measured on the large cylinder radius model and a similar model with a radius a factor of four smaller. The slot height and thus jet half-width were the same with the two models, but the transverse curvature was four times greater on the small cylinder model. Measurements of the shear stress showed no difference in the profiles between the large- and small-radius models. This would indicate that the transverse curvature would have no effect on the shear stress for a straight wall jet. A vortex stretching hypothesis for diverging flows also does not explain a reduction in shear stress. This hypothesis states that, for flows with transverse divergence, vortices with their axes in the transverse direction will get stretched as angular momentum is conserved, and the shear stress will thus increase. This theory has been supported by a limited number of experiments on transversely

diverging flows. The main effect of transverse curvature on the straight wall jet is to cause the outer portions of the jet to diverge, thus having the opposite effect on the shear stress than was observed experimentally.

The effect of transverse convergence or divergence caused by the change in annular radius with downstream distance was studied using the integral method analysis. A major portion of this work was devoted to finding the limits of validity of the approximation of two-dimensional flow with an annular model.

From Fig. 11, it would seem that an annular straight wall jet could simulate the mean flow development of a two-dimensional straight wall jet to high accuracy. However, annular wall jets with streamwise curvature agreed with their two-dimensional counterparts only in the upstream portions of the flow, presumably because transverse curvature effects on the jet became too large far downstream. Two parameters that represent transverse curvature have been identified as $b/r_0$ and $dr_0/dx$. If one of these terms becomes large, transverse curvature will no longer be negligible in the flow. Figure 15 plots computed values of these two terms for a range of annular model geometries. The annular radius at the slot was held constant at 316 slot heights, and the streamwise radius of curvature was varied between 20–1000 slot heights. For each geometry, the mean flow quantities $b(x)/h$ and $U_j^2/U_m^2(x)$ determined by the two-dimensional and annular calculations were compared. The downstream positions where the mean flow agreement was within 5 and 10% was noted on each curve. Subsequently, these points were joined, thus defining boundaries of agreement between two-dimensional and annular flows. The vertical axis in the figure represents the straight wall case, since $dr_0/dx$ would be equal to zero. This line falls entirely within the good agreement region. Mildly curved geometries achieve high values of $b/r_0$ and low values of $dr_0/dx$. The opposite is true for highly curved geometries. The computation for the highly curved geometries was halted when the angular distance along the wall reached 90 deg, and so for extremely high curvatures, this entire flow region would fall into the good agreement portion of the figure. It would be expected that if the transverse radius were increased relative to the slot height, even models with larger streamwise radii of curvature would be able to maintain good mean flow agreement throughout 90 deg of arc.

Further examination of the boundaries of agreement revealed that the product of the two terms $b/r_0$ and $dr_0/dx$ was approximately constant along those boundaries. Therefore, these regions could be described functionally as

$$-\frac{b}{r_0}\frac{dr_0}{dx} < 0.016 \qquad \text{good agreement}$$

$$0.016 < -\frac{b}{r_0}\frac{dr_0}{dx} < 0.032 \qquad \text{moderate agreement}$$

$$0.032 < -\frac{b}{r_0}\frac{dr_0}{dx} \qquad \text{poor agreement}$$

These relations could be used to aid in the design of future annular models, so that regions where two-dimensional flow was satisfactorily approximated could be maximized. For the models used in the present investigation, good agreement occurred over the entire flowfield of the straight wall jet, over the first 90 slot heights of the mildly curved wall jet, and over 26 slot heights of the highly curved wall jet.

The integral momentum analysis also was used to compare the computed shear stresses of the two-dimensional and annular flows. Figures 12–14 show this comparison for the three models. The velocity profiles also were corrected for the annular calculations, although not for the two-dimensional calculations. For the straight wall jet (Fig. 12), the shear stress was self-similar in both computations. There was a slight difference in magnitude, which was entirely accounted for by the velocity profile correction made in one computation and not in the other. If the annular calculation were made without the velocity profile correction, it would overlay the two-dimensional calculation exactly.

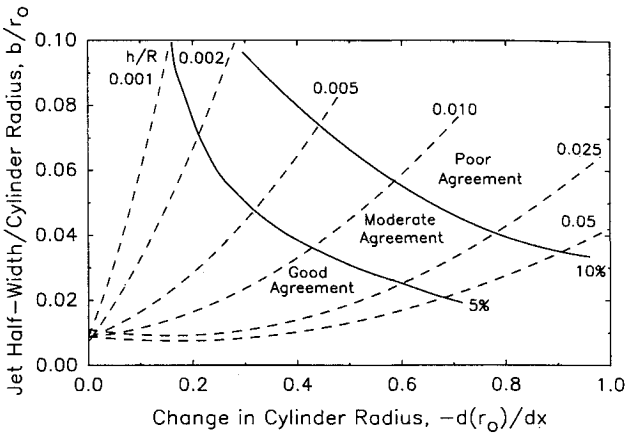


**Fig. 15 Computed boundaries of mean flow agreement between annular and two-dimensional curved wall jets.**

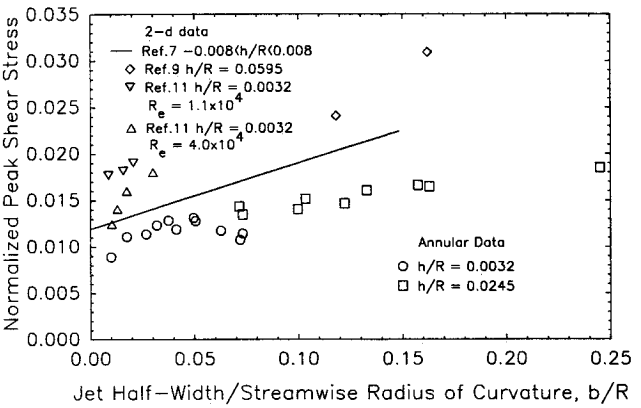


**Fig. 16 Correlation of peak shear stress with streamwise curvature.**

A divergence between the two curves was seen in the curved wall jet cases (Figs. 13 and 14). In each case, the annular computation predicted a higher growth of the peak shear stress than the two-dimensional computation. However, the experimental results did not confirm this result. Since higher streamwise gradients exist in curved wall jets than in straight jets, the thin shear layer approximations made in the analysis may not be valid in the downstream portions of the flow. However, the shear stress results did confirm the regions of agreement found from the mean flow.

Curved wall jets over logarithmic spirals ($R$ is proportional to $x$) have been shown to be self-similar, and the noramlized shear stress results collapse to the same curve, since $b/R$ is a constant at all downstream locations.[8] This raises the possibility that turbulence results on circular arc models also may collapse to the same curve if plotted against $b/R$ rather than $x/h$. It was suggested in Ref. 7 that this was true, and with measurements on circular arcs over a wide range of $h/R$, including concave surfaces, the following empirical relation was found:

$$(\overline{u'v'}/U_m^2)_{\max} = 0.012(1 + 5.8b/R) \qquad (21)$$

This relationship has been compared to the turbulence results found from other researchers investigating circular arc wall jets in Fig. 16. It was seen that, although one or two researchers may find a collapse among data taken on the same experimental rig, there was no agreement between separate

experiments. In Ref. 2, there was no collapse between the two flows at different Reynolds numbers. In the present investigation, the amount of scatter in the curves and the drop in shear stress far downstream in the mildly curved model allowed some leeway in putting a line through the data, and it appeared that a collapse of some sort was possible. Kobayashi and Fujisawa[7] provided the most evidence for a collapse, but their measurements did not agree with anyone else's results. Given the uncertainties present in most of these experiments due to three-dimensionality, it was still inconclusive whether the turbulent shear stress in wall jets over circular arcs would collapse to a single curve when plotted against $b/R$ or whether other parameters such as the Reynolds number need to be accounted for as well.

## Conclusions and Recommendations

An annular wall jet model was chosen in order to achieve a high-quality flow that was free of spanwise nonuniformities. The annular wall jet experiment has been successfully performed with a straight wall, a mildly curved wall, and a highly curved wall. The effects of streamwise curvature on the flowfield, such as the increased growth rate and the increase in the peak shear stress, have been demonstrated.

The integral momentum analysis was able to predict the effects of streamwise curvature on the mean flow in both two-dimensional and annular wall jets. The shear stress in the straight wall jet was also predicted, as long as the appropriate skin friction and velocity profiles were used.

Both the annular model concept and the integral momentum technique have been validated and may be used as test cases for higher-order computational schemes. Recommendations for future work include using the criterion developed for the regions of agreement between annular and two-dimensional flow to design future annular models.

## References

[1]Launder, B. E. and Rodi, W., "The Turbulent Wall Jet," *Progress in Aeronautical Sciences,* Vol. 19, No. 2-4, 1981, pp. 81-128.

[2]Alcaraz, E., Charnay, G., and Mathieu, J., "Measurements in a Wall Jet over a Convex Surface," *Physics of Fluids,* Vol. 20, Feb. 1977, pp. 203-210.

[3]Rodman, L. C., Wood, N. J., and Roberts, L., "An Experimental Investigation of Straight and Curved Annular Wall Jets," Dept. of Aeronautics and Astronautics, Stanford University, Stanford, CA, Rept. JIAA TR-79, Sept. 1987.

[4]Wilson, D. J. and Goldstein, R. J., "Turbulent Wall Jets with Cylindrical Streamwise Curvature," *Journal of Fluids Engineering,* Vol. 98, Sept. 1976, p. 550.

[5]Roberts, L., "A Theory for Turbulent Curved Wall Jets," AIAA Paper 87-0004, 1987.

[6]Cebeci, T. and Bradshaw, P., *Momentum Transfer in Boundary Layers,* McGraw-Hill, New York, 1977.

[7]Kobayashi, R. and Fujisawa, N., "Curvature Effects on Two-Dimensional Turbulent Wall Jets," *Ingenieur-Archiv,* Vol. 53, No. 6, 1983, p. 409-417.

[8]Guitton, D. E. and Newman, B. G., "Self-Preserving Turbulent Wall Jets over Convex Surfaces," *Journal of Fluid Mechanics,* Vol. 81, Pt. 1, 1977, p. 155-185.

[9]Wilson, D. J., "An Experimental Investigation of the Mean Velocity, Temperature and Turbulence Fields in Plane and Curved Two-Dimensional Wall Jets: Coanda Effect," Ph.D. Thesis, Mechanical Engineering Dept., Univ. of Minnesota, Minneapolis, MN, 1970.

[10]McGahan, W. A., "The Incompressible, Turbulent Wall Jet in an Adverse Pressure Gradient," Gas Turbine Lab., Massachusetts Inst. of Technology, Cambridge, MA, Rept. 82, Sept. 1965.

[11]Alcarez, E., "Contribution a l'Etude d'un Jet Plan Turbulent Evoluant le long d'une Paroi Convexe a Faible Courbure," These d'Etat, Univ. Claude Bernard, Lyon, France, 1977.